Radboud Repository

Radboud University Nijmegen

PDF hosted at the Radboud Repository of the Radboud University Nijmegen

The following full text is a publisher's version.

For additional information about this publication click this link.
http://hdl.handle.net/2066/201317

Please be advised that this information was generated on 2021-07-19 and may be subject to change.

Applied Physics Letters

Charge puddles in germanene

Cite as: Appl. Phys. Lett. **114**, 041601 (2019); https://doi.org/10.1063/1.5085304
Submitted: 11 December 2018 . Accepted: 12 January 2019 . Published Online: 28 January 2019

Q. Yao, Z. Jiao, P. Bampoulis, Lijie Zhang, A. N. Rudenko, M. I. Katsnelson, and H. J. W. Zandvliet

View Online Export Citation CrossMark

ARTICLES YOU MAY BE INTERESTED IN

Bandgap opening in hydrogenated germanene
Applied Physics Letters **112**, 171607 (2018); https://doi.org/10.1063/1.5026745

Topographically selective deposition
Applied Physics Letters **114**, 043101 (2019); https://doi.org/10.1063/1.5065801

From 2D to 3D: Graphene molding for transparent and flexible probes
Applied Physics Letters **114**, 043301 (2019); https://doi.org/10.1063/1.5075618

Lock-in Amplifiers up to 600 MHz
starting at $6,210
Zurich Instruments MFLI
Zurich Instruments
Watch the Video

© 2019 Author(s).

AIP Publishing

Applied Physics Letters ARTICLE scitation.org/journal/apl

Charge puddles in germanene

Cite as: Appl. Phys. Lett. **114**, 041601 (2019); doi: 10.1063/1.5085304
Submitted: 11 December 2018 · Accepted: 12 January 2019 · Published Online: 28 January 2019

View Online Export Citation CrossMark

Q. Yao,[1,a)] Z. Jiao,[1,a)] P. Bampoulis,[1] Lijie Zhang,[2,b)] A. N. Rudenko,[3,4,5] M. I. Katsnelson,[4,5] and H. J. W. Zandvliet[1,b)]

AFFILIATIONS

[1] Physics of Interfaces and Nanomaterials, MESA+Institute for Nanotechnology, University of Twente, P.O. Box 217, 7500 AE Enschede, The Netherlands
[2] Hunan Provincial Key Laboratory of Low-Dimensional Structural Physics and Devices, School of Physics and Electronics, Hunan University, Changsha 410082, China
[3] School of Physics and Technology, Wuhan University, Wuhan 430072, China
[4] Radboud University, Institute for Molecules and Materials, Heijendaalseweg 135, 6525 AJ Nijmegen, The Netherlands
[5] Theoretical Physics and Applied Mathematics Department, Ural Federal University, Mira Str. 19, 620002 Ekaterinburg, Russia

[a)] **Contributions:** Q. Yao and Z. Jiao contributed equally to this work.
[b)] **Authors to whom correspondence should be addressed:** lijiezhang@hnu.edu.cn and h.j.w.zandvliet@utwente.nl

ABSTRACT

We report an investigation of the electronic inhomogeneities in a single germanene layer grown on a molybdenum disulfide (MoS_2) substrate. Using scanning tunneling microscopy and spectroscopy, we have recorded spatial maps of the Dirac point of germanene. The Dirac point maps reveal the presence of charge puddles in the germanene sheet. The Dirac point varies from -30 meV to $+15$ meV, corresponding to a charge density in the puddles in the range of 2.6×10^{-3} electrons to 6.6×10^{-4} holes per nm^2. The radius of these puddles is about 10–20 nm, resulting in a total charge of the order of one charge carrier per puddle. The defect concentration in the top layer of the MoS_2 substrate is very comparable to the density of charge puddles, suggesting that the charge puddles are caused by the charged defects in the top layer of the MoS_2 substrate.

Published under license by AIP Publishing. https://doi.org/10.1063/1.5085304

In 2004, Geim, Novoselov, and co-workers managed to isolate a single layer of graphene, i.e., a layer of sp^2 hybridized carbon atoms arranged in a honeycomb structure.[1,2] Graphene is a semimetal with linearly dispersing energy bands at the K and K' points of the Brillouin zone. Owing to these linearly dispersing energy bands, the electrons in graphene behave as massless relativistic particles (see, for instance, Refs. 3 and 4 and references therein). An ideal graphene sheet, i.e., a sheet that is undoped, perfectly flat, and completely free from defects and charged impurities, has its charge neutrality point, also referred to as the Dirac point, located at the Fermi level. The density of states of this ideal graphene sheet vanishes at the Dirac point. Recent experiments have revealed that graphene placed on a substrate often exhibits a spatially varying Dirac point, resulting in electron-hole puddles. The exact origin of these charge puddles is still under debate. Possible candidates for the occurrence of these charge puddles are (1) charged impurities in the substrate on which the graphene is placed,[5,6] (2) charged species which are intercalated between the graphene sheet and the substrate,[7] and (3) the local curvature of the graphene sheet.[8–10]

The first experimental evidence for the occurrence of charge puddles in two-dimensional materials dates back to 2008. Martin *et al.*[5] used a scanning single-electron transistor to spatially map out the charge inhomogeneities in graphene on SiO_2. One year later, Zhang *et al.*[6] used a scanning tunneling microscope to map out the charge density inhomogeneities in graphene on SiO_2 by a technique, referred to as Dirac-point mapping, with a charge density spatial resolution that is substantially higher than what can be achieved by the scanning single-electron transistor. These authors arrived at the conclusion that the electron-hole puddles originate from charge donating defects and/or impurities in the SiO_2 substrate. As demonstrated by Martin *et al.*,[7] also atoms or molecules intercalated between graphene and its support can result in the formation of charge puddles. Gibertini *et al.*[9,10] used density functional theory calculations to show that structural corrugations are in principle sufficient to explain the formation of charge puddles in graphene. They also pointed out that the locations of these electron-hole puddles, which have a typical dimension of a few nanometers, do not exhibit a clear correlation with the

Published under license by AIP Publishing

topography of the graphene sheet. It is worth mentioning that electron-hole puddles are also found in bilayer graphene.[11] So far, charge puddles have only been found in graphene and not in any other elemental two-dimensional material.

The electronic structures of silicon and germanium are very similar to carbon, and therefore, it is worthwhile to check if these materials can form two-dimensional honeycomb lattices. Theoretical calculations have revealed that the graphene-like allotropes of silicon and germanium referred to as silicene and germanene, respectively, are indeed stable.[12–14] Unfortunately, silicene and germanene do not occur in nature, and therefore, these materials have to be synthesized. In 2012, silicene was synthesized,[15,16] followed a few years later by germanene.[17–20] Initially, metallic substrates, particularly transition metal (111) surfaces, were used as templates. In order to electronically decouple the relevant electronic states of the two-dimensional material, which are located near the Fermi level, a bandgap substrate is required. A suitable substrate would be MoS_2, a material with a bulk bandgap of about 1.3 eV. Earlier work revealed that the unique electronic properties of graphene are preserved if MoS_2 is used as a substrate.[21] Inspired by this success, Zhang *et al.* have grown germanene on MoS_2.[22] Scanning tunneling spectroscopy measurements revealed that the density of states of germanene synthesized on MoS_2 exhibits a V-shaped density of states, which is one of the hallmarks of a two-dimensional Dirac material.

In this work, we have investigated the electronic disorder of germanene sheets grown on bulk MoS_2 by using scanning tunneling microscopy. Inspired by the observation of charge puddles in graphene sheets, we have scrutinized if such charge inhomogeneities are also present in germanene. In order to map out the charge density of the germanene sheet, we have used the aforementioned Dirac point mapping technique.

The scanning tunneling microscopy (STM) and spectroscopy (STS) experiments have been performed at room temperature with an ultra-high vacuum STM (Omicron STM-1). The base pressure of the ultra-high vacuum system is 3×10^{-11} mbar. MoS_2 samples were freshly cleaved from synthesized 2H-MoS_2 (purchased from 2D Semiconductors) before inserting into the vacuum system. The MoS_2 samples are mounted on a Mo sample holder. Germanium was deposited onto the MoS_2 substrate, which was held at room temperature, by resistively heating a small piece of a Ge(001) wafer at a temperature of ~1150 K. Prior to the deposition process, the Ge(001) wafer was cleaned by outgassing at a temperature of 700 K for about 24 h followed by several cycles of argon ion bombardment at 800 eV and annealing at 1100 K.[23] The Ge source was located at a distance of ~10 mm from the MoS_2 substrate. After the deposition of germanium, the MoS_2 sample was inserted into the STM.

MoS_2 is a transition metal dichalcogenide that consists of a covalently bonded Mo layer encapsulated between two S layers. The MoS_2 trilayers are held together by weak Van der Waals bonds. The material is a semiconductor with a bulk bandgap of 1.3 eV. The MoS_2 surface has a hexagonal unit cell with a lattice constant of 0.316 nm. Despite the fact that the lattice constant of MoS_2 is substantially smaller than the lattice constant of germanene, MoS_2 is a good substrate for the growth of germanene owing to the relatively weak Van der Waals interaction between the two materials.

In Figs. 1(a) and 1(b), a large-scale scanning tunneling microscopy image and a scanning tunneling spectroscopy spectrum of the pristine MoS_2 surface are shown. By examining several large-scale scanning tunneling microscopy images, similar to the one shown in Fig. 1(a), we have found a defect density of about $3 \times 10^{-3}\,nm^{-2}$. This defect density, which includes the dark and the dimmer defects shown in Fig. 1(a), compares well with a previous study of the defects of MoS_2 using conductive atom force microscopy by Bampoulis *et al.*[24] The dark features in Fig. 1(a) are defects in the first MoS_2 trilayer, whereas the dimmer features are defects located in the second MoS_2 trilayer.[24] As shown by Bampoulis *et al.*,[24] both the dark and dim defects are electronic in nature since they only show up in conductive atomic force microscopy images and not in topographic atomic force microscopy images.

The differential conductivity spectrum displayed in Fig. 1(b) demonstrates that the MoS_2 substrate has a sizeable bandgap. The defects in MoS_2 have been extensively studied (see, e.g., Ref. 25 and references therein). MoS_2 exhibits n-type and p-type defects, which are explained by sulfur-deficient and sulfur-rich regions, respectively.[25]

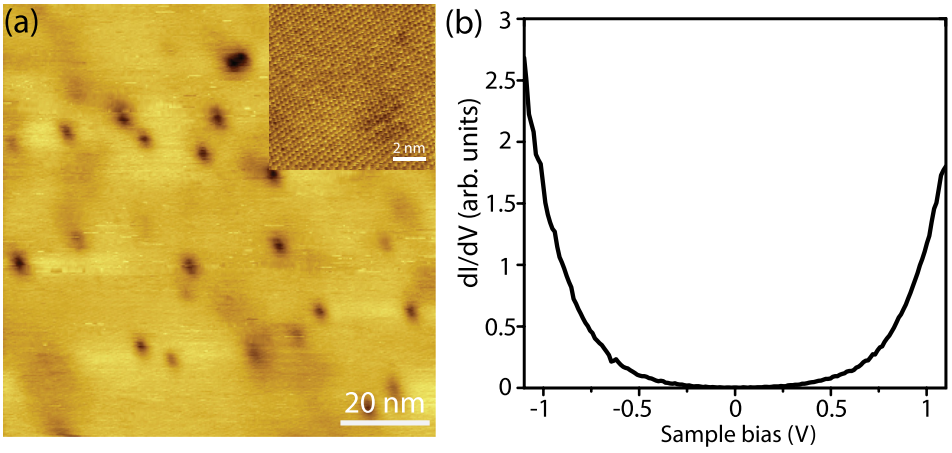

FIG. 1. (a) Scanning tunneling microscopy image of the pristine MoS_2 surface. Inset: small scale scanning tunneling microscopy image. The sample bias is −0.3 V, and the tunnel current is 500 pA. (b) dI/dV spectrum of the pristine MoS_2 surface. The set point values are −1.1 V and 500 pA.

Published under license by AIP Publishing

In Fig. 2(a), a scanning tunneling microscopy image of a germanene layer grown on MoS_2 is shown. As we have already shown in a recent study,[22] Ge atoms deposited on the MoS_2 substrate nucleate at pre-existing defects of the MoS_2 surface. The germanene islands have a height of 3.2 Å and exhibit a hexagonal symmetry with a lattice constant of 3.8–3.9 Å, which is about 20% larger than the lattice constant of pristine MoS_2. This relatively large interlayer spacing of 3.2 Å between the germanene sheet and the MoS_2 substrate hints to a relatively weak interaction between the layers as one expects for materials that are held together by Van der Waals interactions. The deposition of more Ge eventually leads to a complete and very flat germanene layer [see Fig. 2(a)].[22] Owing to the large buckling of germanene on MoS_2, only one of the two triangular sub-lattices is visible in the scanning tunneling microscopy images [see the inset of Fig. 2(a)].

The electronic properties of the germanene layer have been studied by recording grid I(V) curves with the feedback loop disabled. The typical grid size is 60×60 for a 100 nm by 100 nm scan. The differential conductivity (dI/dV), which is proportional to the density of states, is obtained by numerically differentiating the I(V) curves. The averaged dI/dV curve is shown in Fig. 2(b). The differential conductivity displays a V-shape, which is one of the signatures of a two-dimensional Dirac material. The density of states does not completely vanish as the Dirac point. The dI/dV curve is asymmetric, a feature that we have observed before.[22] The asymmetry of the dI/dV curve could be caused by the electronic structure of the STM tip. In addition, it should be noted that the rounded shape near the Dirac point cannot be fully explained by thermal broadening. A much improved fit is, however, obtained by introducing a bandgap of about 25 meV. This bandgap could be due to the presence of a spin-orbit gap in germanene.[26]

Density functional theory calculations shown in Ref. 22 reveal that besides the linear bands at the K and K' points of the Brillouin zone, there are also two parabolic bands in the vicinity of the Fermi level at the Γ point. It is very well possible that these two parabolic bands near the Γ point are responsible for the non-zero density of states at the Dirac point; however, the non-zero density of states could also be caused by the electronic structure of the scanning tunneling microscopy tip.

Since the dI/dV curve shown in Fig. 2(b) is averaged over 3600 different positions on the surface, it is worthwhile to have a detailed look at the spatial variation of the dI/dV curves. In order to do this, we have determined the exact position of the minimum of all individual dI/dV curves. The minimum of the V-shaped dI/dV curve is located at the charge neutrality point, i.e., the Dirac point. As we will show below, the Dirac point provides information on the local charge density. The dispersion relation of a two-dimensional Dirac material is $E = \hbar v_F |k|$, where $\hbar$ is the reduced Planck constant, v_F the Fermi velocity, E the energy of the electron, and k the momentum of the electron. The density of states of a two-dimensional Dirac material is given by

$$D(E) = \frac{2|E - E_D|}{\pi \hbar^2 v_F^2}, \tag{1}$$

where E_D is the Dirac point. The map of the Dirac point can be converted into a map of the charge density by using

$$\rho(x, y) = \int_0^{E_D} \frac{2|E - E_D|}{\pi \hbar^2 v_F^2} dE = -\frac{E_D^2}{\pi \hbar^2 v_F^2} sign(E_D). \tag{2}$$

In Figs. 3(a) and 3(b), spatial maps of the Dirac and charge character of a 100 nm by 100 nm germanene/MoS_2 are shown, respectively. The images consist of 60×60 pixels, and each pixel corresponds to a single I(V) curve. It should be emphasized here that we are dealing with raw data, and we have not applied any smoothening of the I(V) curves in order to determine the minimum of each I(V) curve. The spatial maps of the variation of the Dirac point and charge character reveal that the germanene sheet consists of electron and hole puddles with a typical radius of 10–20 nm embedded in an intrinsic, i.e., undoped, background. The electrostatic screening in two-dimensional Dirac materials is significantly different from electrostatic screening in conventional two-dimensional electron systems. The Dirac point varies from −30 meV to 15 meV corresponding to a charge fluctuation of 2.6×10^{-3} electrons/nm^2 to 6.6×10^{-4} holes/nm^2,

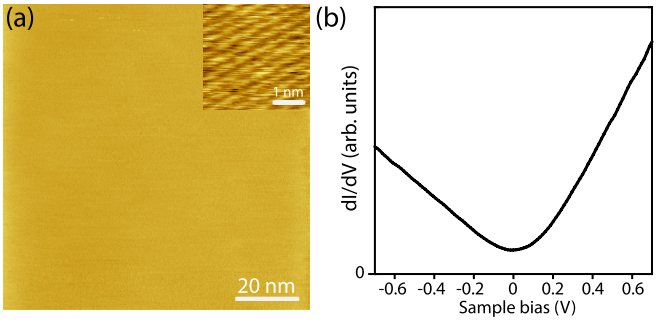

FIG. 2. (a) Large scale scanning tunneling microscopy image (100 nm by 100 nm) of a complete germanene layer grown on MoS_2. Inset: small scale scanning tunneling microscopy image of the germanene layer. The sample bias is −1 V, and the tunnel current is 300 pA. (b) Differential conductivity of germanene. The set point values are −1.4 V and 600 pA.

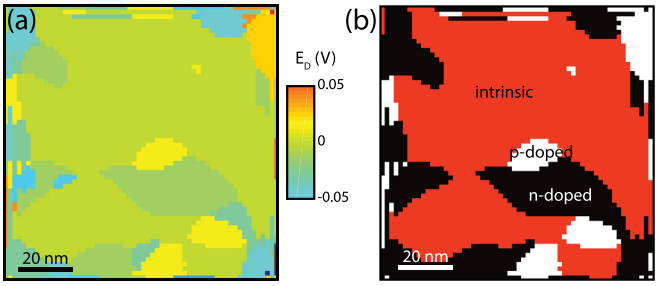

FIG. 3. (a) Spatial map (60×60 pixels) of the Dirac point of germanene/MoS_2. The image size is 100 nm by 100 nm. The color code refers to the position of the Dirac point. (b) Spatial map (60×60 pixels) of the charge character of germanene/MoS_2 (red: intrinsic, black: n-type, and white: p-type). The image size is 100 nm by 100 nm.

Published under license by AIP Publishing

assuming a Fermi velocity of 5×10^5 m/s.[27] Since the germanene sheet is atomically flat on a length scale exceeding the typical size of the charge puddles, we have to rule out the possibility that charge puddles are caused by structural corrugations or bending of the germanene sheet. The germanene sheet is grown and subsequently studied at ultra-high vacuum conditions, and therefore, we can also rule out the intercalation of atoms or molecules as being the cause of the charge puddles. The only remaining sources are charge donating impurities in the MoS_2 substrate. By analyzing several large-scale scanning tunneling microscopy images of our pristine and freshly cleaved MoS_2 substrate, we find a defect density of $3 \times 10^{-3}\,nm^{-2}$. This value compares favorably well with the charge puddle density we have determined for the germanene sheet. Based on these findings, we suggest that the charge puddles are caused by charge donating defects of the MoS_2 substrate.

The typical radius of the charge puddles in germanene is about 10–20 nm. A crude estimate for the size of the charge puddle is the Thomas-Fermi screened length. In conventional two-dimensional electron systems, the density of states in energy space is constant, and therefore, the Thomas-Fermi screening length, which is inversely proportional to the density of states at the Fermi level, is constant.[28–31] In two-dimensional Dirac systems, however, the density of states is proportional to the energy. This results in a Thomas-Fermi screening length of $2\pi\kappa\hbar v_F/4e^2\sqrt{\pi n}$, where n is the charge density.[28] Assuming a Fermi velocity of 5×10^5 m/s (Refs. 27 and 32) and a charge density of $\sim 3 \times 10^{-3}\,nm^{-2}$ (one charge carrier per defect), we find for germanene on molybdenum disulfide a Thomas-Fermi length of ~10 nm, which is somewhat smaller than our experimental observations. In addition, the size of the charge puddles in germanene is very comparable to the size of the charge puddles found in graphene at a comparable charge density (see Ref. 6). Please note that the charge density in Ref. 7 is substantially larger than in our case and Ref. 6, resulting in, as expected, smaller charge puddles.

In a previous study,[22] we found a qualitative good agreement between the dI/dV spectrum and the density functional theory calculations. There is, however, an overall energy shift of about 0.3 eV between the experimental and theoretical spectra. In Ref. 22, we tentatively ascribed this energy shift to the presence of defects and/or impurities with an acceptor character. In this work, we have not found any evidence for the presence of these acceptor types of defects and/or impurities in the germanene layer, and therefore, we have to discard this interpretation.

In conclusion, we have studied the charge inhomogeneities of germanene grown on MoS_2. The charge fluctuations in germanene have been mapped out by using a Dirac point map. Spatial maps of the Dirac point and the charge character reveal that the germanene sheet consists of electrons and hole puddles with a typical radius of 10–20 nm embedded in an intrinsic, i.e., undoped, background. The typical charge per puddle is of the order of one electron or hole. The defect density of MoS_2 is determined by the analysis of several large-scale scanning tunneling microscopy images and compares very well with the charge density of the germanene sheet. We found strong indications that the charge puddles in germanene are caused by charge-donating defects and impurities in the MoS_2 substrate. Our results demonstrate that even in van der Waals heteroepitaxy, the quality of the substrate plays a key role. Charge donating defects or impurities result in electronic inhomogeneities in the two-dimensional material.

This work is part of the research programme on 2D semiconductor crystals with Project No. FV157-TWOD, which is financed by the Netherlands Organization for Scientific Research (NWO). Q.Y. and Z.J. thank the China Scholarship Council for financial support. L.Z. also thanks the Fundamental Research Funds for the Central Universities from China. A.N.R. acknowledges the support from the Russian Science Foundation under Grant No. 17-72-20041.

REFERENCES

[1]K. S. Novoselov, A. K. Geim, S. V. Morozov, D. Jiang, Y. Zhang, S. V. Dubonos, I. V. Grigorieva, and A. A. Firsov, Science **306**, 666 (2004).
[2]A. K. Geim and K. S. Novoselov, Nat. Mater. **6**, 183 (2007).
[3]A. H. Castro Neto, F. Guinea, N. M. R. Peres, K. S. Novoselov, and A. K. Geim, Rev. Mod. Phys. **81**, 109 (2009).
[4]M. I. Katsnelson, *Graphene: Carbon in Two Dimensions* (Cambridge University Press, Cambridge, 2012).
[5]J. Martin, N. Akerman, G. Ulbricht, T. Lohmann, J. H. Smet, K. von Klitzing, and A. Yacoby, Nat. Phys. **4**, 144 (2008).
[6]Y. Zhang, V. W. Brar, C. Girit, A. Zettl, and M. E. Crommie, Nat. Phys. **5**, 722 (2009).
[7]S. C. Martin, S. Samadar, B. Sacépé, A. Kimouche, J. Coraux, F. Fuchs, B. Grévin, H. Courois, and C. B. Winkelmann, Phys. Rev. B **91**, 041406(R) (2015).
[8]A. Deshpande, W. Bao, F. Miao, C. N. Lau, and B. J. LeRoy, Phys. Rev. B **79**, 205411 (2009).
[9]M. Gibertini, A. Tomadin, M. Polini, A. Fasolino, and M. I. Katsnelson, Phys. Rev. B **81**, 125437 (2010).
[10]M. Gibertini, A. Tomadin, F. Guinea, M. I. Katsnelson, and M. Polini, Phys. Rev. B **85**, 201405 (2012).
[11]G. M. Rutter, S. Jung, N. N. Klimov, D. B. Newell, N. B. Zhitenev, and J. A. Stroscio, Nat. Phys. **7**, 649 (2011).
[12]K. Takeda and K. Shiraishi, Phys. Rev. B **50**, 14916 (1994).
[13]G. G. Guzmán-Verri and L. C. Lew Yan Voon, Phys. Rev. B **76**, 075131 (2007).
[14]S. Cahangirov, M. Topsakal, E. Aktürk, H. Şahin, and S. Ciraci, Phys. Rev. Lett. **102**, 236804 (2009).
[15]P. Vogt, P. De Padova, C. Quaresima, J. Avila, E. Frantzeskakis, M. C. Asensio, A. Resta, B. Ealet, and G. Le Lay, Phys. Rev. Lett. **108**, 155501 (2012).
[16]A. Fleurence, R. Friedlein, T. Ozaki, H. Kawai, Y. Wang, and Y. Yamada-Takamura, Phys. Rev. Lett. **108**, 245501 (2012).
[17]L. Li, S.-Z. Lu, J. Pan, Z. Qin, Y.-Q. Wang, Y. Wang, G. Cao, S. Du, and H.-J. Gao, Adv. Mater. **26**, 4820 (2014).
[18]M. E. Dávila, L. Xian, S. Cahangirov, A. Rubio, and G. Le Lay, New J. Phys. **16**, 095002 (2014).
[19]P. Bampoulis, L. Zhang, A. Safaei, R. van Gastel, B. Poelsema, and H. J. W. Zandvliet, J. Phys. Condens. Matter **26**, 442001 (2014).
[20]A. Acun, L. Zhang, P. Bampoulis, M. Farmanbar, M. Lingenfelder, A. van Houselt, A. N. Rudenko, G. Brocks, B. Poelsema, M. I. Katsnelson, and H. J. W. Zandvliet, J. Phys. Condens. Matter **27**, 443002 (2015).
[21]B. Sachs, L. Britnell, T. O. Wehling, A. Eckmann, R. Jalil, B. D. Belle, A. I. Lichtenstein, M. I. Katsnelson, and K. S. Novoselov, Appl. Phys. Lett. **103**, 251607 (2013).
[22]L. Zhang, P. Bampoulis, A. N. Rudenko, Q. Yao, A. van Houselt, B. Poelsema, M. I. Katsnelson, and H. J. W. Zandvliet, Phys. Rev. Lett. **116**, 256804 (2016).
[23]H. J. W. Zandvliet, Phys. Rep. **388**, 1 (2003).
[24]P. Bampoulis, R. van Bremen, Q. Yao, B. Poelsema, H. J. W. Zandvliet, and K. Sotthewes, ACS Appl. Mater. Interfaces **9**, 19278 (2017).

Published under license by AIP Publishing

[25]R. Addou, L. Colombo, and R. M. Wallace, ACS Appl. Mater. Interfaces **7**, 11921 (2015).
[26]C.-C. Liu, W. Feng, and Y. Yao, Phys. Rev. Lett. **107**, 076802 (2011).
[27]C.-C. Liu, H. Jiang, and Y. Yao, Phys. Rev. B **84**, 195430 (2011).
[28]S. Das Sarma, S. Adam, E. H. Hwang, and E. Rossi, Rev. Mod. Phys. **83**, 407 (2011).
[29]S. Samaddar, I. Yudhistira, S. Adam, H. Courois, and C. B. Winkelmann, Phys. Rev. Lett. **116**, 126804 (2016).
[30]M. I. Katsnelson, Phys. Rev. B **74**, 201401(R) (2006).
[31]R. John and B. Merlin, J. Phys. Chem. Solids **110**, 307 (2017).
[32]M. Ezawa, J. Phys. Soc. Jpn. **84**, 121003 (2015).

Published under license by AIP Publishing